Synthesis and Characterization of Manganese complexes as Photooxidation Catalysts

Estudiant: David Morea Martín   Grau en Biotecnologia

Correu electrònic: david.morea.martin@gmail.com

Tutor: Mª Isabel Romero

Empresa / institució: Universitat de Girona

Vistiplau tutor:

Nom del tutor: Mª Isabel Romero

Empresa / institució: Universitat de Girona

Correu(s) electrònic(s): marisa.romero@udg.edu

Data de dipòsit de la memòria a secretaria de coordinació:

Index

Summary

This project has consisted in the synthesis of five manganese complexes containing the N-bidentate ligand 2,9-dimethyl-1,10-phenanthroline, *dmp*, together with two monodentate ligands, -Cl and -CF$_3$SO$_3$, the study of their spectroscopic, structural and electrochemical properties, and their evaluation as catalysts for the photooxidation of alcohols into aldehydes and ketones.

The first three synthesized complexes were obtained by a process of mixing the reagents, stirring, filtrating the medium, and washing it. These three catalysts were [MnCl$_2$(dmp)$_2$] **1**, [Mn$_2$Cl$_4$(dmp)$_2$] **2** and [Mn(CF$_3$SO$_3$)$_2$(dmp)$_2$] **4**. From the crystallization of compound **2**'s mother liquor compound [MnCl$_2$(dmp)(H$_2$O)] **3** was obtained. On the other hand, recrystallization of complex **4** in an ethyl acetate solution produced crystals of [Mn(OAc)(dmp)(OH$_2$)$_2$](dpmH)(CF$_3$SO$_3$)$_2$ **5**. All five compounds were subsequently characeried through IR spectroscopy, cyclic voltammetry, ESI-MS, elemental analysis and X-ray diffraction.

After the characterization of the five catalysts, compounds **1**, **2** and **4** and other three additional ones, **1a**, **2a** and **3a**, synthesized during a previous project, were tested as photocatalysts in the oxidation of alcohols. Firstly, a study was made to determine the optimal reaction time, which was found to be 12 h. All the compounds showed moderate yield with high selectivity values for the photooxidation of 1-phenylethanol. The complexes containing the pyridine pyrazole ligand (**1a-3a**) presented better performance than **1-3** complexes, which contained the *dmp* ligand. In general, the yield values displayed by chloride catalysts were higher than those presented by the triflate complexes. Finally, the two chloride complexes, **1** and **2**, were used to catalyze the photooxidations of five different alcohols in neutral and acidic media.

The last phase of the project was dedicated to demonstrate the formation of high valent manganese species in water when Mn(II) is oxidized by a compound with a higher redox potential such as [Ru^{III}(bpy)$_3$]$^{3+}$. This was visualized by UV-Vis and ESI-MS spectroscopy and accomplished by both photooxidation and chemical oxidation.

Resum

El present treball de fi de grau ha consistit en la síntesi de cinc complexes de manganès a partir del lligand N-bidentat 2,9-dimetil-1,10-fenantrolina, *dmp*; i de dos lligands mono-dentats, -Cl i -CF$_3$SO$_3$. A partir d'ells s'ha estudiat les seves propietats espectroscòpiques, estructurals i electroquímiques, i s'ha avaluat la seva activitat catalítica per a la foto-oxidació d'alcohols en aldehids i cetones.

Els tres primers complexes en sintetitzar-se van ser obtinguts per un procés de mescla dels reactius, agitació, filtració del medi, i rentat del mateix. Aquests tres catalitzadors van ser [MnCl$_2$(dmp)$_2$] **1**, [Mn$_2$Cl$_4$(dmp)$_2$] **2** i [Mn(CF$_3$SO$_3$)$_2$(dmp)$_2$] **4**. A partir de la cristal·lització de les aigües mare del complex **2** es va obtenir el complex [MnCl$_2$(dmp)(H$_2$O)] **3**, i la recristal·lització del complex **4** en solució d'acetat d'etil va donar lloc a cristalls de [Mn(OAc)(dmp)(OH$_2$)$_2$](dpmH)(CF$_3$SO$_3$)$_2$ **5**. Tots cinc compostos van ser posteriorment caracteritzats a través d'espectroscòpia IR, voltametria cíclica, ESI-MS, anàlisi elemental i difracció per raigs X.

Després de la caracterització dels cinc catalitzadors, els compostos **1**, **2** i **4** i altres tres d'addicionals: **1a**, **2a** i **3a**, sintetitzats en un treball anterior, van ser estudiats per avaluar la seva capacitat per a oxidar alcohols. Al principi es va realitzar una prova per determinar el temps òptim de reacció, que va resultar ser de 12 hores. Després de realitzar les reaccions pertinents, els resultats van mostrar rendiments moderats i alta selectivitat en tots els complexes per a la fotooxidació d'1-feniletanol. Els complexes que contenien el lligand piridina-pirazola (**1a-3a**) van comportar-se millor que els complexes **1-3**, que contenien en canvi el lligand *dmp*. En general, els rendiments donats pels catalitzadors amb lligand cloro eren majors que els presentats pels que tenien lligand triflat. Finalment es van estudiar els dos clor complexes, **1** i **2**, com a catalitzadors en la fotooxidació de diferents alcohols en medi neutre i àcid.

La darrera fase del projecte es va dedicar a demostrar la formació en aigua de compostos de manganès en alts estats d'oxidació quan el Mn(II) és oxidat per un compost amb un potencial redox més alt com ara el [Ru^{III}(bpy)$_3$]$^{3+}$. Els resultats van ser visualitzats per espectroscòpia UV-Vis i ESI-MS I aconseguits per fotooxdiació I oxidació química.

Resumen

El presente trabajo de fin de grado ha consistió en la síntesis de cinco complejos de manganeso a partir del ligando N-bidentado 2,9-dimetil-1,10-fenantrolina, *dmp*; y de dos ligandos mono-dentados, -Cl y -CF$_3$SO$_3$. A partir de ellos se han estudiado sus propiedades espectroscópicas, estructurales i electroquímicas, i se ha evaluado su actividad catalítica para la fotooxidación de alcoholes en aldehídos y cetonas.

Los tres primeros complejos fueron obtenidos a partir de la mezcla de los reactivos, agitación, filtración del medio, y lavado del mismo. Estos tres catalizadores fueron [MnCl$_2$(dmp)$_2$] **1**, [Mn$_2$Cl$_4$(dmp)$_2$] **2** y [Mn(CF$_3$SO$_3$)$_2$(dmp)$_2$] **4**. A partir de la cristalización de las aguas madre del complejo **2** se obtuvo el complejo [MnCl$_2$(dmp)(H$_2$O)] **3**, y la recristalización del complejo **4** en solución de acetato de etilo dio lugar a cristales de [Mn(OAc)(dmp)(OH$_2$)$_2$](dpmH)(CF$_3$SO$_3$)$_2$ **5**. Los cinco compuestos fueron posteriormente caracterizados a través de espectroscopia IR, voltametría cíclica, ESI-MS, análisis elemental y difracción por rayos X.

Tras la caracterización de los cinco catalizadores, los compuestos **1**, **2** y **4** y otros tres adicionales: **1a**, **2a** y **3a**, sintetizados en un trabajo anterior, fueron estudiados para evaluar su capacidad para oxidar alcoholes. Inicialmente, se determinó el tiempo óptimo de reacción, que resultó ser de 12 horas. Después de realizar las reacciones pertinentes, los resultaros mostraron rendimientos moderados y alta selectividad en todos los complejos para la fotooxidación de 1-feniletanol. Los complejos que contenían el ligando piridina-pirazola (**1a-3a**) se comportaron mejor que los complejos **1-3**, que contenían en cambio el ligando *dmp*. En general, los rendimientos dados por los catalizadores con ligando cloro eran mayores que los presentados por los que tenían ligando triflato. Finalmente se estudiaron los dos cloro complejos, **1** y **2**, como catalizadores de la fotooxidación de distintos alcoholes en medio neutro y ácido.

La última fase del proyecto se dedicó a demostrar la formación en agua de compuestos de manganeso en altos estados de oxidación, cuando Mn(II) es oxidado por un compuesto con un potencial redox más alto como[Ru^{III}(bpy)$_3$]$^{3+}$. Los resultados fueron visualizados por espectroscopía UV-Vis y ESI-MS y fueron realizados mediante fotooxidación y oxidación química.

1. Introduction

Alcohol oxidations are one of the most common reactions in organic chemistry. Depending on the type of alcohols, they give rise to aldehydes, carboxylic acids or ketones. The variety of generated products make them an important source for intermediates and building blocks. For their obtaining, catalytic reactions are much more efficient than stoichiometric ones.

1.1. Catalysis

Catalysis is a process in which the rate of approaching the thermodynamic equilibrium of a chemical reaction is accelerated by a compound that is not consumed: the catalyst. It can be described as a cyclic event where the catalyst participates but is recovered in its original form at the end of the process. Nowadays, catalysis is essential in chemistry, since it is required for the synthesis of many chemicals. Approximately 85-90% of the chemical industry products are produced with at least one catalytic reaction.

Catalysis can be categorized as homogeneous or heterogeneous, depending on the relationship between the phase of the catalyst and the involved reactants. This project has focused on homogeneous catalysis.

To discuss catalysis, this project will mainly use the following terms:

Conversion

The conversion is the ratio between the moles of reactant consumed and the moles of reactant introduced in the reaction. To calculate conversion equation 1 is used:

$$Conversion = \frac{moles\ of\ reactant\ consumed}{moles\ of\ reactant\ introduced\ in\ the\ reaction} \quad (1)$$

Yield

The yield in one product is the ratio between the moles of the product formed and the moles of reactant introduced in the reaction. Its calculation is shown in equation 2:

$$Yield = \frac{moles\ of\ product\ formed}{moles\ of\ reactant\ introduced\ in\ the\ reaction} \quad (2)$$

Selectivity

The selectivity of a reaction (Equation 3) is the ratio between the yield and the conversion. This concept is useful when other by-products are generated in a reaction.

$$Selectivity = \frac{moles\ of\ reactant\ consumed\ to\ form\ the\ desired\ product}{total\ moles\ of\ ractant\ consumed} = \frac{Yield}{Conversion}\ (3)$$

1.2. Transition-metal complexes

The need to search for more efficient catalysts has brought the possibility of transition-metal complexes. These types of catalysts are formed by nitrogen-based ligands coordinated with a first-row transition metal such as manganese. Their suitability is explained by their rich coordination chemistry, simple synthesis, and inexpensiveness of first-row transition metals.

Concerning manganese-containing complexes, the most investigated systems are the ones based on sp2-hybridized nitrogen-donor atoms such as chiral oxazolines or pyridines, porphyrines and Salen ligands. While manganese complexes containing bipyridine and derivatives have given good results on alkene epoxidation catalysis, similar ligands such as neocuproine have never been studied as catalysts in oxidation reactions.

1.3. Manganese in catalysis

1.3.1. Biomimetic reactions

Many enzymes are present in Nature acting as "biological catalysts" capable of catalyzing oxidation reactions in living organisms[1]. Metals in enzymes participate in complex biochemical reactions and highly specialized biological functions thanks to their ability to exist in multiple oxidation states and different geometries. Manganese compounds are used as biomimetic catalyst due to its biological role. Manganese is an essential trace nutrient in all forms of life. Traces of manganese are found in many plants and bacteria, and a healthy human adult contains about 10-20mg of Mn. The classes of enzymes that have manganese cofactors are very broad, and include oxidoreductases, transferases, hydrolases, lyases, isomerases, ligases, lectins, and integrins. The reverse transcriptases of many retroviruses contain manganese. The best-known manganese-containing polypeptides may be arginase, the diphtheria toxin, and Mn-containing superoxide dismutase (Mn-SOD).

These enzymes are frequently studied by using model complexes which provide information on the nature and reactivity of the active site and about possible reaction mechanisms. Several factors modulate the reactivity of the active center, such as the nature of the metal and the ligand or the coordination geometry of the metal center. Based on the manganese or iron containing enzymes and on the related model complexes various oxidation catalysts have been evaluated.

These enzymes are frequently studied by using model complexes which provide information on the nature and reactivity of the active site and about possible reaction mechanisms. Several factors modulate the reactivity of the active center, such as the nature of the metal and the ligand or the coordination geometry of the metal center. Based on the manganese or iron containing enzymes and on the related model complexes various oxidation catalysts have been evaluated.

1.3.2. Oxidation of substrates

The development of technologies for production of chemical fuels or useful compounds with renewable energy (e.g. sunlight) and inexpensive feedstocks relies on an abundant supply of protons and electrons to form the reduced products. In natural oxygenic photosynthesis, a possible blueprint for artificial photosynthesis, the only suitable abundant source for the needed protons and electrons is water. Oxidation of water liberates protons and electrons and gives off oxygen gas.

The main problem of oxidation reactions is that they are both thermodynamically and kinetically demanding, resulting in slow kinetics without the use of a catalyst.

Oxidation of substrates mediated by transition metals is a reaction of great interest from a chemical and biological point of view. Specifically, oxidation of olefins, alcohols, amines and sulphides, among others, is interesting from an academic and industrial point of view, because of the corresponding products play an important role as intermediates and building blocks in synthesis and materials science[2].

Therefore, one of the challenges of this century is to design catalysts to improve the control of the activity and selectivity of chemical processes and at the same time be compatible and respectful with the environment. Light can be considered an ideal reagent for environmentally friendly, green chemical synthesis. Unlike many conventional reagents, visible light is non-toxic, generates no waste and can be obtained from renewable sources. Also, it is an abundant source of energy for driving chemical reactions. Solar energy combined with water is the good alternative energy sources for the development of non-fossil based fuel.[3] Photocatalysts are powerfully enabling in synthetic applications because they absorb light and convert the energy absorbed into chemical potential used to transform organic and inorganic substract.

During the last decades, a series of homogeneous catalysts were found to be active in oxidation reactions. In this project, efficient manganese catalysts for chemical oxidation reactions have been developed. From the perspective of the sustainability the research and develop of efficient systems, it is essential to understand at molecular level the reactions involved in oxidation processes and induced by light.

Oxidation of alcohols is a thermodynamically uphill conversion that involves a two electron-two proton coupled process[4]. This process has a practical importance in hydrogen-based energy technologies because of the anodic liberation of protons and electrons that can be coupled on a cathode for hydrogen fuel production in an integrated photoelectrochemical cell.

$$RCH(\text{-}OH)R' \longrightarrow RC(=O)R' + 2\ H^+ + 2\ e^- \quad (4)$$
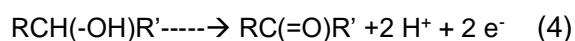
The few studies related to the visible light-driven alcohol oxidation have been performed using chromophore-catalyst dyad of manganese complexes[5], one performing as a photosensitizer and the second as a catalyst.

1.3.3. Manganese in biological systems

In living organisms, manganese(II) ions are the required cofactor for many ubiquitous enzymes. For instance, the ATP-dependent Ca transporter located in mitochondria can accumulate Mn^{2+} ions, and its functioning can regulate cellular respiration or mediate apoptosis. The transport based on Mn(II) ions can be taken advantage of for developing tumor-targeted compounds.

Several Mn(II)-based complexes have been synthesized and reported to have antitumoral activities against leukemia cancer cell line, HeLa cells[6], human hepatoma cells, and human gastric cancer cell lines. In general, Mn(II) complexes containing pyridine rings have shown antibacterial activities and DNA-binding properties and could give promising results as anticancer agents.

2. Objectives

The aims of this work are the ones following:

- Learn the techniques of synthesis and spectroscopic and electrochemical characterization, characteristic of an inorganic chemistry research laboratory.

- Synthesis and characterization of new Mn^{II} compounds containing the ligand 2,9-dimethyl-1,10-phenanthroline, *dmp*, together with two monodentate ligands, -Cl and -CF_3SO_3.

- Study the catalytic performance of these new complexes along with other previously studied in the literature, in the photooxidation of alcohols in water, using $[Ru(bpy)_3]Cl_2$ as a photosensitizer and $Na_2S_2O_8$ as sacrificial oxidant.

- Study of the formation of High-Valent manganese species in water by UV-visible and ESI-MS spectroscopy.

3. Experimental Section

3.1. Instrumentation and measurements

IR spectra were recorded on an Agilent Cary 630 FTIR spectrometer equipped with an ATR MK-II Golden Gate Single Reflection system. UV-Vis spectroscopy was performed on a Cary 50 Scan (Varian) UV-Vis spectrophotometer with 1 cm quartz cells. Cyclic Voltammetry (CV) and Differential Pulse Voltammetry (DPV) experiments were performed in an IJ-Cambria 660C potentiostat using a three-electrode cell. Glassy carbon electrode (3 mm diameter) from BAS was used as working electrode, platinum wire as auxiliary and SCE as the reference electrode. The complexes were dissolved in solvents containing the necessary amount of n-Bu$_4$N+PF$_6^-$ (TBAH) as supporting electrolyte to yield a 0.1 M ionic strength solution. All $E_{1/2}$ values reported in this work were estimated from cyclic voltammetric experiments as the average of the oxidative and reductive peak potentials (E_{pa}+E_{pc})/2, or directly from DPV. Unless explicitly mentioned the concentration of the complexes was approximately 1mM. The NMR spectroscopy was performed on Bruker 400 MHz ASCEND spectrometers. Samples were run in CD$_2$Cl$_2$ or CDCl$_3$. Elemental analyses were performed using a CHNS-O Elemental Analyser EA-1108 from Fisons. ESI-MS experiments were performed on a Navigator LC/MS chromatograph from Thermo Quest Finnigan, using acetonitrile as mobile phase.

Crystallographic Data Collection and Structure Determination
Measurement of the crystals were performed on a Bruker Smart Apex CCD diffractometer using graphite-monochromated Mo Kα radiation (λ = 0.71073Å) from an X-Ray tube. Data collection, Smart V. 5.631 (BrukerAXS 1997-02); data reduction, Saint+ Version 6.36A (Bruker AXS 2001); absorption correction, SADABS version 2.10 (Bruker AXS 2001) and structure solution and refinement, structure solution and refinement, SHELXL-2013 (Sheldrick, 2013).

3.2. Synthesis of compounds

Materials. All reagents used in the experimental work were obtained from Sigma-Aldrich Co and were not further purified. Reagent grade organic solvents were obtained from Carlo Erba and high purity de-ionized water was obtained by passing distilled water through a nano-pure Mili-Q water purification system.

Preparations

Preparation of [MnCl$_2$(dmp)$_2$] (1): A solution of neocuproine (0.182 g, 0.874 mmol) and MnCl$_2$ (0.050 g, 0.397 mmol) in acetonitrile (5 mL) was stirred for 30 min at room temperature. The obtained white precipitate was collected by filtration and then washed with diethyl ether and dried in air. A portion of it was dissolved in CH$_2$Cl$_2$ *for crystallization*. After a week, the evaporation of CH$_2$Cl$_2$ left crystals of **1**, suitable for X-ray diffraction analysis. Yield: 0.111 g (51.6%). Anal. Found (Calc.) for C$_{28}$H$_{24}$Cl$_2$MnN$_4$: C, 60.41 (59.96); H, 4.24 (4.64); N, 10.10 (9.99) %. IR (cm^{-1}): υ = 3000-3100 (υ (NH)); 1600 (υ (C-N)sp^2); 1433 (υ (C-C)sp^2) cm^{-1}. $E_{1/2}$ (III/II): 0.85 V vs. SCE. ESI-MS (m/z): 439 [MnCl$_2$(dmp)(CH$_3$CN)$_2$Na$^+$].

Preparation of [Mn$_2$Cl$_4$(dmp)$_2$] (2) and [MnCl$_2$(dmp)(H$_2$O)] (3): A solution of neocuproine (0.108 g, 0.509 mmol) and MnCl$_2$ (0.028 g; 0.222 mmol) of in ethanol (5 mL) was stirred for 30 min at room temperature. A white precipitate was obtained and collected by filtration. Then, the solid was washed with diethyl ether, and dried in air. A portion of it was dissolved in CH$_2$Cl$_2$ for crystallization. After a week, the evaporation of CH$_2$Cl$_2$ left crystals of **2**, suitable for X-ray diffraction analysis. The mother liquor of **2**, which had also been left evaporating, produced crystals of **3**. **The following data corresponds to compound 2:** Yield: 0.081 g (67.5%). Anal. Found (Calc.) for C$_{28}$H$_{24}$Cl$_4$Mn$_2$N$_4$: C, 49.61 (49.54); H, 3.69 (3.26); N, 8.27 (8.30) %. IR (cm^{-1}): υ = 3106-3000-3100 (υ (NH)); 1600 (υ (C-N)sp^2); 1433 (υ (C-C)sp^2) cm^{-1}. $E_{1/2}$ (III/II): 0.89 V vs. SCE. ESI-MS (m/z): 479 [Mn$_2$Cl$_4$(dmp)(H$_2$O) H$^+$]$^+$.

Preparation of [Mn(CF$_3$SO$_3$)$_2$(dmp)$_2$] (4): A solution of neocuproine (0.061 g, 0.874 mmol) and 0.050 g (0.397 mmol) of Mn(CF$_3$SO$_3$)$_2$ in THF (5 mL) was stirred for one hour at room temperature. Afterwards, the obtained pale-yellow precipitate was filtered off, washed with diethyl ether, and dried in air. A portion of it was dissolved in CH$_2$Cl$_2$ for crystallization. After a week, the evaporation of CH$_2$Cl$_2$ left crystals of **4**, suitable for X-ray diffraction analysis. Yield: 0.069 g (22.5%). Anal. Found (Calc.) for C$_{30}$H$_{24}$F$_6$MnN$_4$O$_6$S$_2$: C, 46.16 (45.75); H, 3.37 (2.96); N, 7.17 (7.27) %. IR (cm^{-1}): υ = 3000-3100 (υ (NH)); 1600 (υ (C-N)sp^2); 1433 (υ (C-C)sp^2) cm^{-1}. Anodic Peak Potential: 0.99 V. ESI-MS (m/z): 620 [Mn(CF$_3$SO$_3$)(dmp)$_2$]$^+$.

Obtaining of [Mn(OAc)(dmp)(OH$_2$)$_2$](dpmH)(CF$_3$SO$_3$)$_2$ (5): by recrystallization of 4 in an ethyl acetate solution, yellow needles suitable for X-ray diffraction were obtained corresponding to complex 5.

Photocatalytic oxidation studies

For the majority of samples, a glass vessel containing 3 mL of phosphate buffer pH 6.8 or acetate buffer pH 4, depending on the case, together with the corresponding catalyst (0.5 mM), $[Ru(bpy)_3]^{2+}$ (5 mM) as photosensitizer, substrate (50 mM) and $Na_2S_2O_8$ (100 mM) as sacrificial acceptor was stirred under N_2 and exposed to continuous irradiation with a xenon lamp (150, Hamamtsu L8253), equipped with a 400-700 nm large band filter, for 12 hours. The resulting solution was extracted with CH_2Cl_2 for three times. The solvent was evaporated under reduced pressure. The reaction product was characterized by ^{1}H NMR spectroscopy.

3.3.   Ethical and sustainability criteria

Nowadays, the strive to reduce waste and improve efficiency continues under the principles of green chemistry. Many traditional reactions are experiencing transformations in order to meet sustainability criteria. One of the main objectives in chemistry is to avoid the use of uncommon reactants and prioritize the abundant or renewable ones. For this reason, photo redox catalytic systems based on an earth abundant metal like manganese would be a good approach to sustainability.

The present project has used catalytic reactions instead of stoichiometric ones, satisfying one of the principles of Green Chemistry[7]. However, important solvent amounts were used for the synthesis of the complexes and the extraction of the reactions' products, and none of the reagents came from a renewable source. What is more, while atomic economy was high considering substrate-to-product atoms, photosensitizers and sacrificial oxidants could not be recovered.

In spite of these drawbacks, for the preparation of samples the used product quantities were as small as possible. In addition, generated residues were properly stored in the corresponding containers.
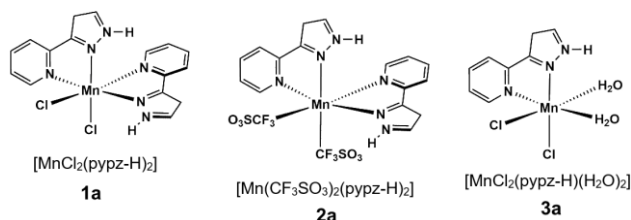
4. Results and Discussion

4.1.   Synthesis of the complexes

The strategy followed to synthesize Mn[II] complexes **1-5** is outlined in Scheme 1. For the preparation of complexes **1a**, **2a** and **3a**, the synthetic route described in the literature[8] was followed (see Scheme 2).
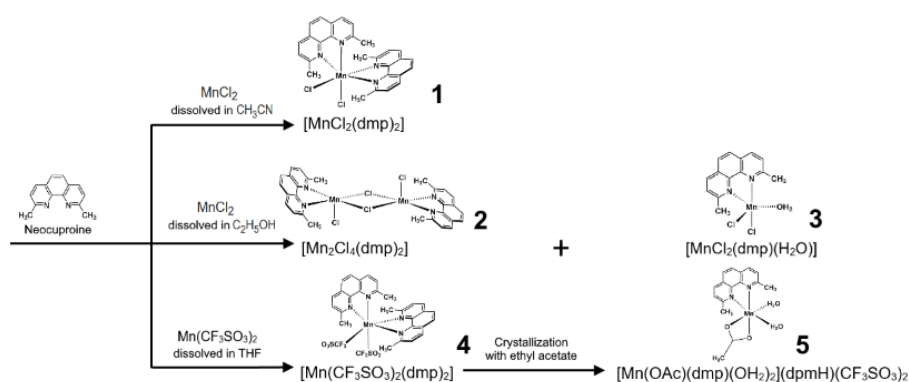
Scheme 1. Synthetic strategy for the synthesis of complexes **1-5**.

Scheme 2. Drawing of the complexes **1a-3a** used in this work.

As what can be seen in Scheme 1, by adding neocuproine, *dmp*, to an acetonitrile solution with MnCl$_2$ dissolved and with a metal:ligand ratio 1:2.2, the complex [MnCl$_2$(dmp)$_2$], **1**, is obtained in good yield and it can be crystallized in a CH$_2$Cl$_2$ solution. However, if the solvent is ethanol, despite using the same ratio, [MnCl$_2$(dmp)$_2$]$_2$, **2**, containing chloride bridged ligands, is otherwise produced. By slow evaporation of the mother liquor, the monomeric complex [MnCl$_2$(dmp)(OH$_2$)], **3**, is obtained by crystallization. The same metal:ligand ratio of 1:2.2 can also be used to obtain the mononuclear compound [Mn(CF$_3$SO$_3$)$_2$(dmp)$_2$], **4**, starting from the corresponding Mn(CF$_3$SO$_3$)$_2$ salt. Finally, the recrystallization of complex 4 in the presence of ethyl acetate resulted in the formation of the complex [Mn(OAc)(dmp)(OH$_2$)$_2$](dpmH)(CF$_3$SO$_3$)$_2$, **5**. In this case, the hydrolysis of the solvent takes place with the coordination of the acetate, as a bidentate ligand, to the manganese (II), together with two aqua ligands that replace the two triflate ligands, that now act as counterions together with one protonated *dmp* ligand.

4.2.   Structural characterization

Crystal structures of the five Mn(II)-containing synthesized complexes containing the N-bidentate ligand, *dmp*, have been solved by X-diffraction analysis. Main crystallographic data and selected bond distances and angles for compounds **1-5** are presented in Tables 1-5. ORTEP plots with the corresponding atom labels for their X-ray structure are presented in Figures 1-5.

Complex 1

Figure 1 shows the molecular structure, while Table 1 displays bond distances and bond angles.
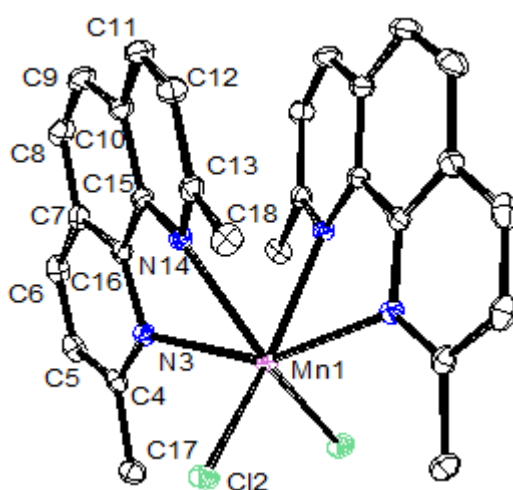
Figure 1. Ortep structure for complex **1**.

Table 1. Selected bond lengths (Å) and angles (°) for complex **1**.

Mn—N(3)	2.3085(12)	N(3) —Mn—Cl(2)	99.70(3)
Mn—Cl(2)	2.4428(7)	Cl(2) —Mn—N(14)	91.44(4)
Mn—N(14)	2.4539(12)	N(14) —Mn—N(3)	69.15(4)

The picture above shows that the Mn metal center adopts a distorted octahedral type of coordination. Two of the coordination sites are occupied by chloride ligands, and the other four sites are occupied by four N atoms of the two bidentate *dmp* ligands.

Complex 2

Crystal structures obtained for the mononuclear compound **1** and the dinuclear compound **2** are similar to the previously described in the literature[9]. In this case, the dinuclear compound **2** co-crystallizes with mononuclear [MnCl$_2$(dmp)(dmf)] compound. In this project, compound **2** crystallizes alone.
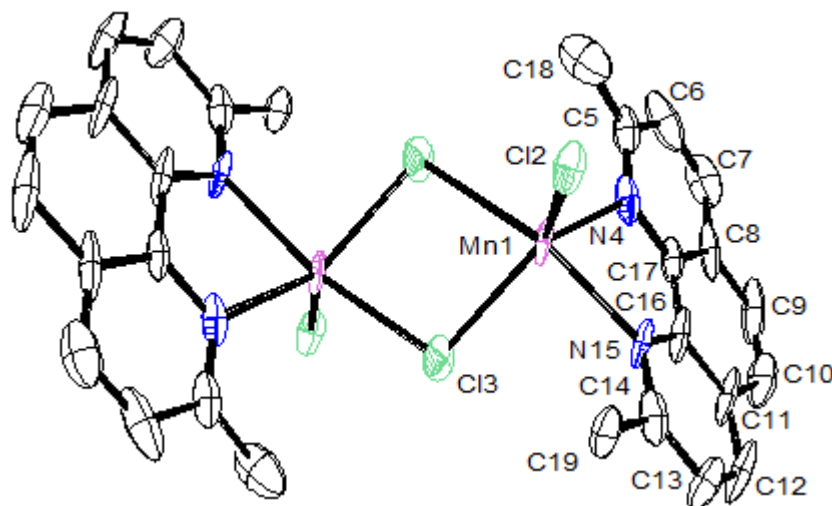
Figure 2. Ortep structure for complex **2**.

Table 2. Selected bond lengths (Å) and angles (°) for complex **2**.

Mn—N(15)	2.224(9)	N(4)—Mn—Cl(2)	113.6(3)
Mn—Cl(2)	2.312(5)	N(4)—Mn—Cl(3)	127.4(3)
Mn—Cl(3)	2.490(5)	N(15)—Mn—Cl(2)	107.3(3)
Mn—N(4)	2.235(10)	Cl(2)—Mn—Cl(3)	118.71(19)
N(15)—Mn—N(4)	74.0(4)	N(15)—Mn—Cl(3)	85.7(3)

Complex **2** contains two pentacoordinate manganese (II) ions, which are bridged by two chloride ligands. The other three positions around each metal are occupied by two nitrogen of the *dmp* ligand and a terminal chlorine atom, (Figure X). The geometry around each manganese is a distorted square pyramid: the two nitrogen atoms of the *dmp* ligand and the two chloride bridges constitute the bases, and the apical positions are occupied by the two terminal chloride ligands. Both manganese atoms are equivalent since the complex has a rotational C2 symmetry axis passing through the centre of their core. The Mn-Mn bond length (3.763 Å), the Mn-Cl bridging bond lengths (2.463 and 2.490 Å) and the terminal Mn-Cl bond lengths (2.313 Å) are close to those of other structurally characterized Mn^{II}Mn^{II} di-μ-chloro complexes[10].

Complex 3

Complex **3** displays a distorted trigonal bipyramid around the Mn(II) ion, where the equatorial plane is occupied by the two monodentate chloride ligands, and one nitrogen atom, N(16) of the bidentate dmp. The apical positions involve the other nitrogen atom N(5) of the *dmp* ligand and the oxygen atom O(4) of the aqua ligand.
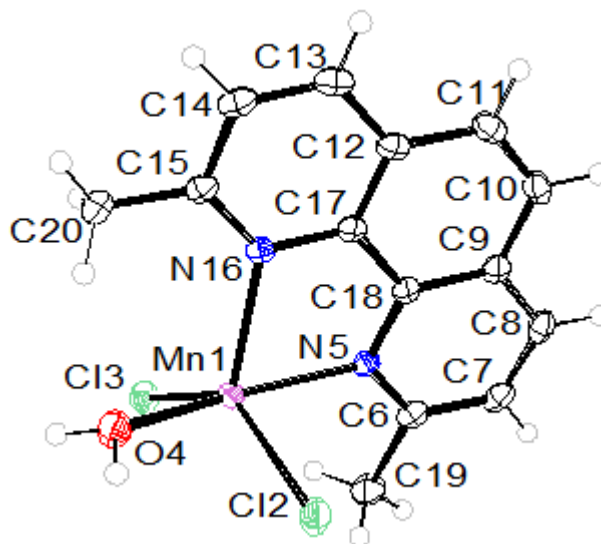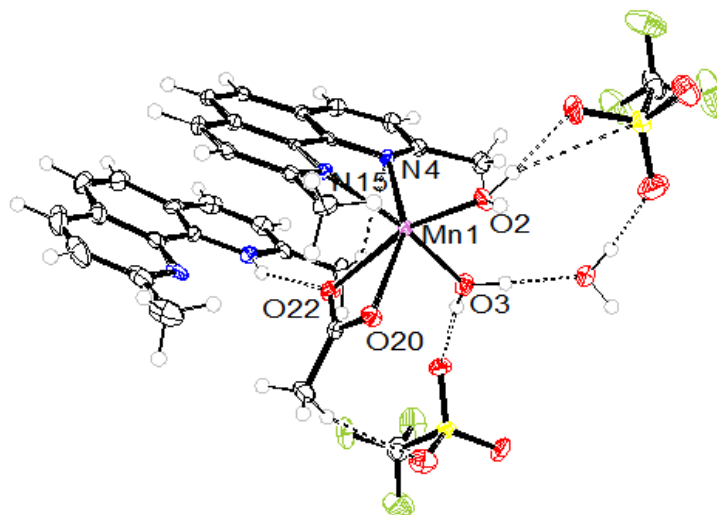

Figure 3. Ortep structure for complex **3**.

Table 3. Selected bond lengths (Å) and angles (°) for complex **3**.

Mn—O(4)	2.103(5)	O(4) —Mn—Cl(3)	104.61(17)
Mn—N(16)	2.040(5)	N(16) —Mn—Cl(3)	174.38(15)
Mn—N(5)	2.076(4)	N(5) —Mn—Cl(3)	95.99(18)
Mn—Cl(3)	1.952(4)	O(4) —Mn—Cl(2)	94.14(13)
Mn—Cl(2)	2.081(4)	N(16) —Mn—Cl(2)	91.48(16)
O(4) —Mn—N(16)	2.396(3)	N(5) —Mn—Cl(2)	99.34(16)
N(16) —Mn—N(5)	77.03(17)	Cl(3) —Mn—Cl(2)	92.38(17)

Compared to the idealized trigonal bipyramid, the angles between the Mn atom and the ligands show significant distortions. The spatially constrained nature of the bidentate dmp ligand produces geometrical distortions manifested in the N(5)–Mn–N(16) angle equal to 75.18º compared to 90º the theoretical value (Table S). Other distortion is observed in the O(4)–Mn–N(5) angle corresponding to the apical positions, whose value is of 162.07º compared to the theorical 180º. The bond lengths show the same tendency as other complexes described in the literature.[11]

13

Complex 4

The mononuclear complex **4** displays a distorted trigonal prismatic geometry around the metal. There, the Mn(II) ion is coordinated by four nitrogen atoms of two *dmp* ligands and two oxygen atoms from the anionic monodentate triflate ligands, adopting a *cis* configuration around the metal. In this structure the two ligands are almost coplanar with an intramolecular length between phenanthroline rings of 3.27 Å, similar to other compounds described in the literature. O-Mn-N/O angles for adjacent atoms and angles formed between the atoms that form the diagonal of the prism's rectangular faces are in accordance with a prismatic trigonal geometry[12].
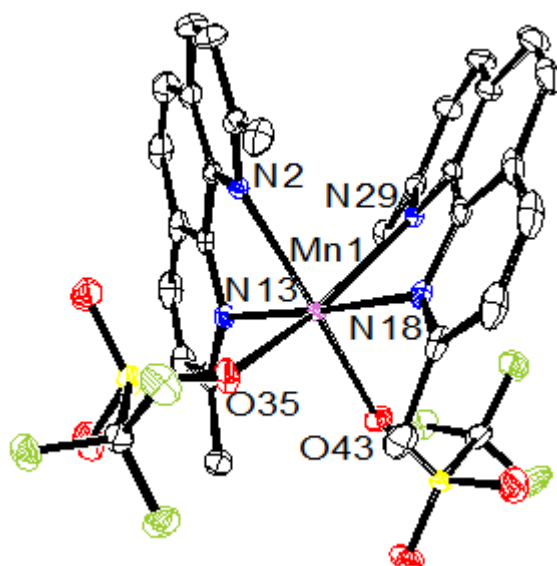
Figure 4. Ortep structure for complex **4**.

Table 4. Selected bond lengths (Å) and angles (°) for complex **4**.

Mn—O(43)	2.127(2)	**O(43) —Mn—O(35)**	98.88(9)
Mn—O(35)	2.296(2)	**O(35) —Mn—N(18)**	90.84(8)
Mn—N(2)	2.296(2)	**O(43) —Mn—N(13)**	90.32(7)
Mn—N(13)	2.132(2)	**O(43) —Mn—N(18)**	91.97(7)
Mn—N(18)	2.304(2)	**N(18) —Mn—N(13)**	175.36(7)
Mn—N(29)	2.315(2)	**O(35) —Mn—N(13)**	92.80(7)

Complex 5

Finally, compound **5** shows a highly distorted octahedral coordination geometry around the Mn(II) ion. It is coordinated by two nitrogen atoms of the *dmp* ligand, two oxygen atom of the acetate ligand, and two oxygen atoms of the terminal aqua ligands, disposed in a cis position. The high distortion observed is due to the spatially constrained nature of the bidentate *dmp* and acetate ligands, and both N(4)–Mn–N(15) and O(20)–Mn–O(22) angles (74.62º and 57.27º respectively) are below the theoretical value of 90º.

Figure 5. Ortep structure for complex **5**.

Table 5. Selected bond lengths (Å) and angles (°) for complex **5**.

Mn—O(2)	2.103(2)	O(2) —Mn—O(3)	90.72(10)
Mn—O(20)	2.242(3)	O(3) —Mn—O(20)	88.51(10)
Mn—N(15)	2.280(3)	O(3) —Mn—N(4)	97.67(10)
Mn—O(3)	2.176(3)	O(2) —Mn—O(15)	103.83(10)
Mn—N(4)	2.250(3)	O(20) —Mn—N(15)	91.33(10)
Mn—O(22)	2.349(3)	O(2) —Mn—O(22)	159.50(9)

The structure also contains intramolecular H-bonding interactions between the H(24) of the protonated *dmp* ligand and O(22) atom of the acetate ligand (2.075 Å) and π-stacking interaction between the two phenanthroline rings (3.44 Å) (Figure). Other H-bonding interactions are observed between the aqua ligands and the triflate anions, O(3S)-H(3A) = 1.999 Å and O(3R)-H(2B) = 1.919 Å.

4.3.   Spectroscopic properties

4.3.1. IR spectroscopy

Figures 6 and 7 below show the IR spectra corresponding to complexes **1** and **4**. One common feature of the two complexes is that around 2800-3000 cm^{-1} both of them show peaks corresponding to the vibration υ(=C-H), which are part of the aromatic ligands. Another shared characteristic can be seen around 1600 cm^{-1}, where the peaks represent the υ(C=N) stretching of the aromatic ligands. In figure 7, between 1200 and 1400 cm^{-1}, several peaks corresponding to the stretching vibration of triflate ($CF_3SO_3^-$) bonds are visible. Lastly, even though not easily distinguishable, the peaks corresponding to deformations and aliphatic tensions of C-H bonds around 1400 cm^{-1} appear in all spectra.
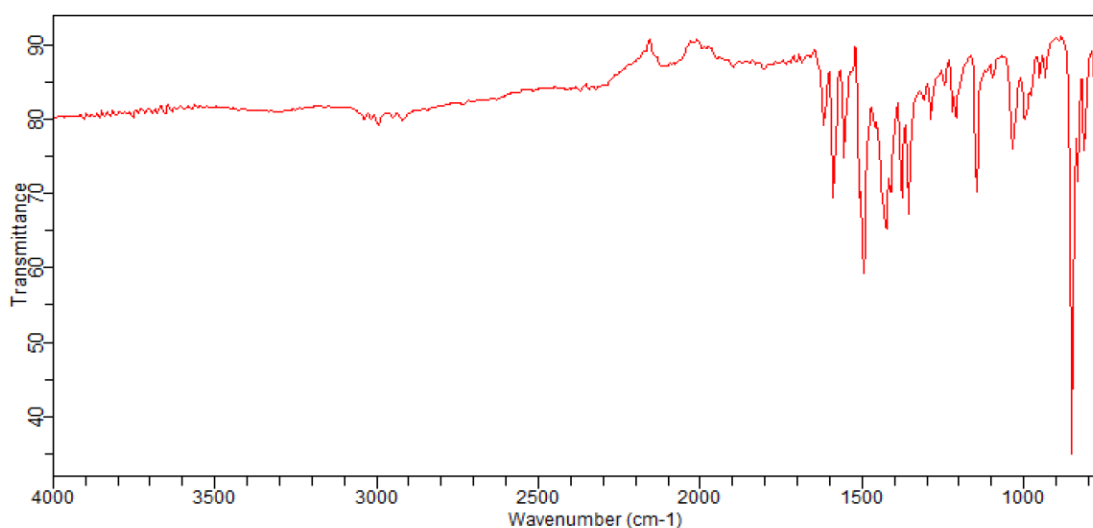
Figure 6. IR spectra of complex **1**.
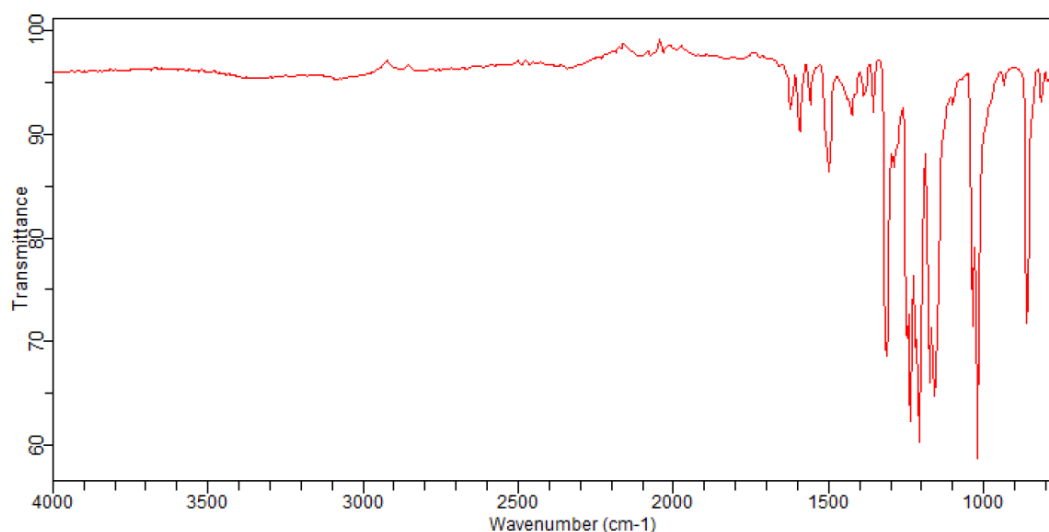
Figure 7. IR spectra of complex **4**.

16

4.4.   Electrochemical properties

The redox potentials of complexes **1, 2** and **4** were investigated through cyclic voltammetry (CV) in CH_3CN containing 0.1 M of $n\text{-}Bu_4NPF_6$ (TBAH) as supporting electrolyte and SCE as the reference electrode. The voltammograms obtained are shown in Figures 8-10.

Voltammograms of complexes **1** and **2** (Figures 9 and 10) exhibit a one-electron quasi-reversible redox wave at potential values of $E_{1/2}$ = 0.85 V (**1**) and 0.89 V (**2**) corresponding to the Mn^{III}/Mn^{II} system. In both compounds, a new wave is observed at 0.92 V for complex **1** and 1.06 V for complex **2**. Those phenomena are related to the presence of new Mn(II) species arising from the substitution of Cl ligands by acetonitrile solvent, and the increase in the $E_{1/2}$ value with regard to the initial wave would be in accordance with the higher electron-withdrawing ability of CH_3CN when compared to chloride ligands[13].

In contrast, for triflate compound **4**, CV experiments display irreversible oxidation processes at $E_{p,a}$ = 0.99 V (Figure 10, Table 6). This compound is oxidised at a higher potential than the structurally similar chlorido complex **1**, which can be explained in terms of the stronger electron-donating capacity of chlorido ligands compared to the above-mentioned anions. Compound 4 is probably irreversible because of the instability of generated Mn(III) species by oxidation, which probably turn into other molecules that cannot be reduced.
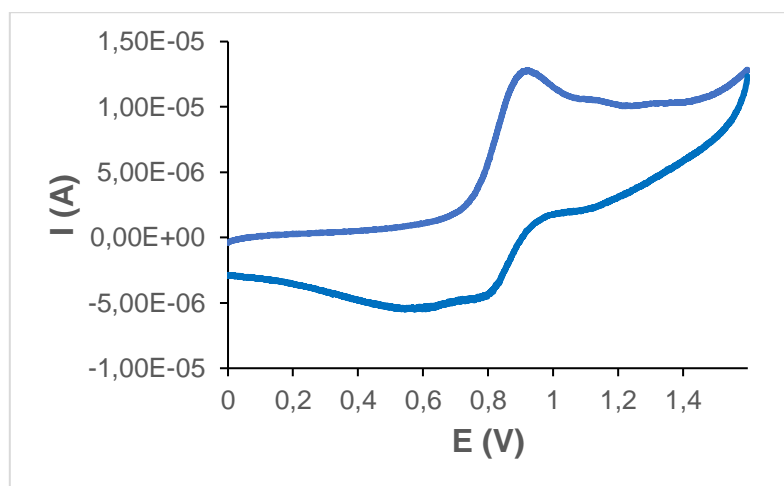
Figure 8. CV for complex **1**, registered in CH_3CN +0.1M TBAP with SCE as the reference electrode.
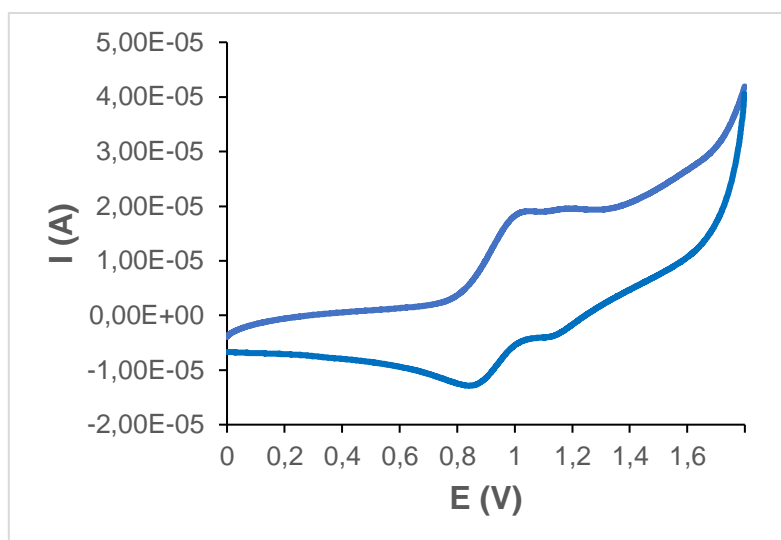
Figure 9. CV for complex **2,** registered in CH$_3$CN +0.1M TBAP with SCE as the reference electrode.
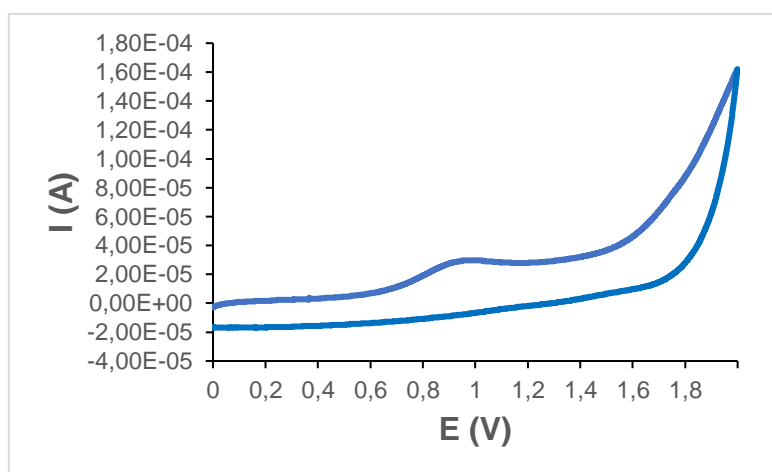
Figure 10. CV for complex **4**, registered in CH$_3$CN +0.1M TBAP with SCE as the reference electrode.

Table 6. Electrochemical data (E$_{1/2}$ in V vs SCE) and redox reactions for Mn complexes studied in this project. [a]Corresponds to an anodic peak potential.

entry	compound	$E_{1/2}$ (III/II)	redox reaction
1	**1**	0.85	**[Mn^{II}Cl(dmp)$_2$]** $\rightleftharpoons$ **[Mn^{III}Cl$_2$(dmp)$_2$] + e$^-$**
2	2	0.89	**[Mn$_2$^{II}Cl$_4$(dmp)$_2$]** $\rightleftharpoons$ **[Mn$_2$^{III}Cl$_4$(dmp)$_2$] + e$^-$**
3	4	0.99[a]	**[Mn^{II} (CF$_3$SO$_3$)$_2$(dmp)$_2$]** $\rightarrow$ **[Mn^{III} (CF$_3$SO$_3$)$_2$(dmp)$_2$] + e$^-$**
4	Ru(bpy)$_3$Cl$_2$	1.03	**[Ru^{II}(bpy)$_3$Cl$_2$]$^{2+}$** $\rightleftharpoons$ **[Ru^{III}(bpy)$_3$Cl$_2$]$^{3+}$ + e$^-$**

4.5.   Catalytic experiments

4.5.1.   Catalytic photooxidation of alcohols

From the CV observed in Figure 11, the reduction potential of $[Ru(bpy)_3]^{3+}$(1V *vs* SCE) in a phosphate buffer (pH 6.8) solution is more positive than the oxidation potential of $Mn^{III/II}$ for complex **1**. Therefore, the PCET oxidation of **1** by the photogenerated $[Ru(bpy)_3]^{3+}$ is thermodynamically favourable and the photocatalytic oxidation should take place.
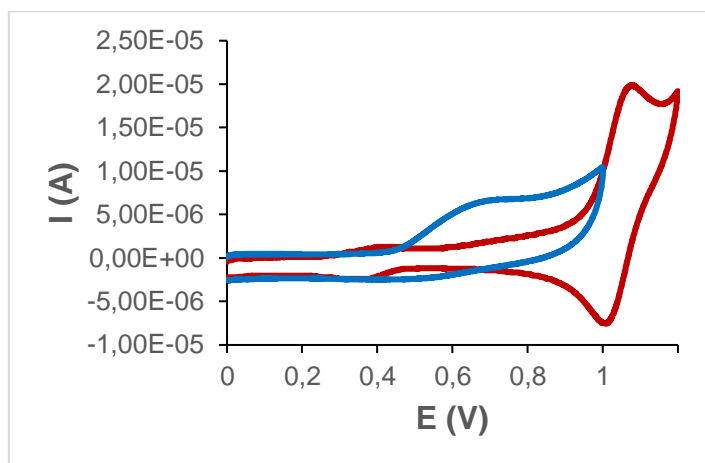
Figure 11. Comparison of CV voltammetries for $Ru(bpy)_3Cl_2$ (red) and complex **2** (blue), registered in phosphate buffer pH 6.8 with SCE as the reference electrode.

On most of the samples, the relationship between the components in the reaction medium was 1:10:100:200. Specifically, the concentrations of each reagent were 0.5 mM for the manganese catalyst, 5 mM for the photosensitizer, Tris(bipyridine)ruthenium(II) chloride ($[Ru(bpy)_3]Cl_2$); 50 mM for sodium persulfate ($Na_2S_2O_8$); and 100 mM for the alcohol substrate. All four were dissolved in 3 mL of phosphate buffer pH 6.8 or acetate buffer pH 4, depending on the case.

Firstly, different reaction times were probed using 1-phenylethanol as the subtract, in order to optimize the reaction time on the photocatalytic oxidation experiments. Table 7 shows the evolution of the yields vs. time, where the yield obtained for the sample with 24 h of reaction time did not increase significantly with respect to the sample with 12 hours of reaction time. For this reason, this time was chosen as optimal to perform the catalytic experiments. Under dark conditions and with all reagents in the reaction pot, after 12 h of reaction, no significant oxidation of alcohol occurred (below 2%) and in the absence of catalyst or oxidizing agent but with exposure to light, the oxidation of alcohols was below 4%. In all cases, aldehyde or ketone was detected as the unique product of the oxidation reaction, being the selectivity achieved > 99%.

Table 7. Mn-catalyzed 1-phenylethanol oxidation[a] by complex one measured by three reaction times.
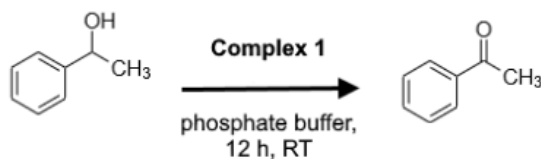
Reaction time (h)	Yield (%)
7	29
12	51
24	56

[a]Oxidation conditions: **1**: [Ru(bpy)$_3$]Cl$_2$:1-phenylethanol: Na$_2$S$_2$O$_8$ (catalyst/photosensitizer/substrate/oxidant) ratio of 1:10:100:200 in phosphate buffer pH 6.8, 12 h at RT.

On the first phase of the study, catalytic complexes **1**, **2**, **4**, **1a**, **2a** and **3a** were all tested for their oxidation of the same substrate, 1-phenylethanol and Table 8 displays the catalytic results obtained.

Table 8. Mn-catalyzed 1-phenylethanol oxidation[a].
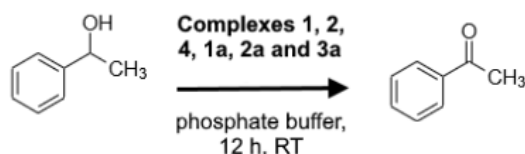
Catalyst	Yield (%)	Catalyst	Yield (%)
	51		59
	48		55
	41		64

[a]Oxidation conditions: **1, 2 4, 1a, 2a, 3a**: [Ru(bpy)$_3$]Cl$_2$:1-phenylethanol: Na$_2$S$_2$O$_8$ (catalyst/photosensitizer/substrate/oxidant) ratio of 1:10:100:200 in phosphate buffer pH 6.8, 12 h at RT.

As we can see in Table 8, all the compounds show moderate yield with high selectivity values for the photooxidation of 1-phenylethanol. the complexes containing the pyridine pyrazole ligand (**1a-3a**) present better performance than **1-3** complexes, which contain the *dmp* ligand and in general, the yield values displayed by chloride catalysts are higher than those presented by the triflate complexes. The differences observed can be explained by slower oxidation kinetics for the triflate compounds since the oxidation potential of the chlorido complexes are significantly lower than those of triflate complexes. Also, distinctive high-valent species are probably involved depending on the pre-catalyst used.

After these experiments, the availability of complexes **1a-3a** was limited, so, for this reason, the next phase of the catalytic study was firstly studied using complex **1**, which had the best performance out of the three tested complexes that were synthesized during this project.

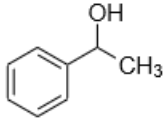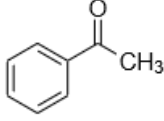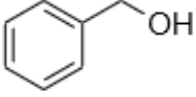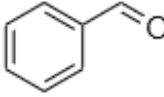**Table 9.** Complex **1**-catalyzed oxidation of different alcohols.
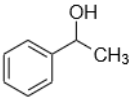
Substrate	Product	Yield (%)
1-phenylethanol	1-phenylethanone	51
Benzyl alcohol	Benzaldehyde	52
4-methylbenzyl alcohol	4-methylbenzaldehyde	58
4-chlorobenzyl alcohol	4-chlorobenzaldehyde	48
Diphenylmethanol	Benzophenone	68
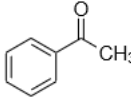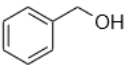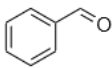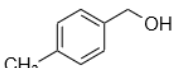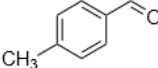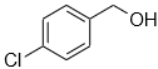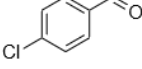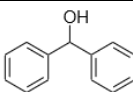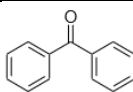
[a]Oxidation conditions: **1**: [Ru(bpy)$_3$]Cl$_2$:alcohol: Na$_2$S$_2$O$_8$ (catalyst/photosensitizer/substrate/oxidant) ratio of 1:10:100:200 in phosphate buffer pH 6.8, 12 h at RT.

Table 9 displays the catalytic results obtained in the photooxidation of different alcohols by complex **1**. These results show moderate yields in aldehyde and ketones. For the primary alcohols, the yield is enhanced by the presence of electron-donating substituents on the aromatic ring of the benzylalcohol (entry 3) but is decreased by the presence of electron withdrawing substituents, as chloro (entry 4). These results are in accordance with the presence of electrophilic species as intermediates.

With the idea to investigate the behaviour of the compounds as catalysts in a wide pH range, we have also performed the oxidation reactions in acetate buffer (pH 4), using complexes **1** and **2** as catalysts and using similar conditions to the previously described. Table 10 shows the obtained results.

Table 10. Complex **1** and complex **2**-catalyzed oxidation of 4 alcohols at pH 4.

Substrate	Product	Yield (%), Complex 1	Yield (%), Complex 2
 1-phenylethanol	 1-phenylethanone	55 (51)[b]	67 (48)
 Benzyl alcohol	 Benzaldehyde	61 (52)	29
 4-methylbenzyl alcohol	 4-methylbenzaldehyde	-	68
 Diphenylmethanol	 Benzophenone	-	44
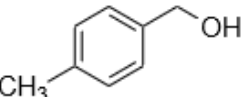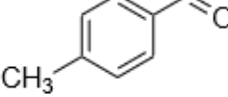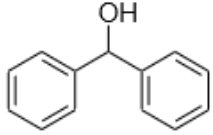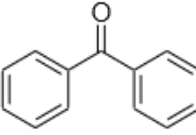
[a]Oxidation conditions: **1, 2**: [Ru(bpy)$_3$]Cl$_2$:alcohol: Na$_2$S$_2$O$_8$ (catalyst/photosensitizer/substrate/oxidant) ratio of 1:10:100:200 in acetate buffer pH 4, 12 h at RT. [b] in parentheses are given the obtained values a pH 6.8.

As it can be seen in Table 10, in general the yields improve with acetate buffer pH 4 in comparison with when phosphate buffer pH 6.8 is used. The 68% yield obtained for the oxidation of 4-methylbenzyl alcohol is the highest that has been seen for a newly synthesized catalyst in the entire catalytic study. This behaviour could be presumably due to the less stability of the active intermediate species on higher pH 6.8.

## 4.6. UV-Vis spectroscopy for the study of the formation of High-Valent manganese species in water

UV-Vis and ESI-MS spectroscopy were performed to demonstrate that Mn^{II} complexes are oxidized into Mn^{III} and Mn^{IV} species when they are oxidized by a compound with a higher redox potential such as $[Ru^{III}(bpy)_3]^{3+}$. In these studies, complex **4** $[Mn^{II}(CF_3SO_3)_2(dmp)_2]$ was used. In the first test, this was accomplished by photocatalytic oxidation , and in the second by chemical oxidation.

The first experiment consisted in the photocatalytic generation of high-valent manganese species by preparing 2 mL of solution containing complex **4** (1.0 mM), $[Ru^{III}(bpy)_3]^{2+}$ (0.5 mM), and $[Na_2S_2O_8]$ (5.0 mM) all mixed in an Ar-degassed acetate buffer (pH 4.0, 50 mM) and MeCN (v/v 1:6) mixed solvent. The solution was exposed to irradiation of a Xe lamp light source (300 W) with a cut-off filter ($\lambda > 420$ nm) while being stirred at 273 K. After 10 min of exposure, the reaction solution was put in ice and immediately measured again in the spectrometer.

The second experiment consisted in the chemical generation of the above-mentioned species. In this case was required the preparation of a 2 mL reaction solution with the same solvent and the same concentration of complex **4**, but without the addition of $[Ru^{III}(bpy)_3]^{2+}$ and $[Na_2S_2O_8]$. Instead, ammonium cerium(IV) nitrate, a strong oxidizing agent, was added with a concentration of 4.0 mM.

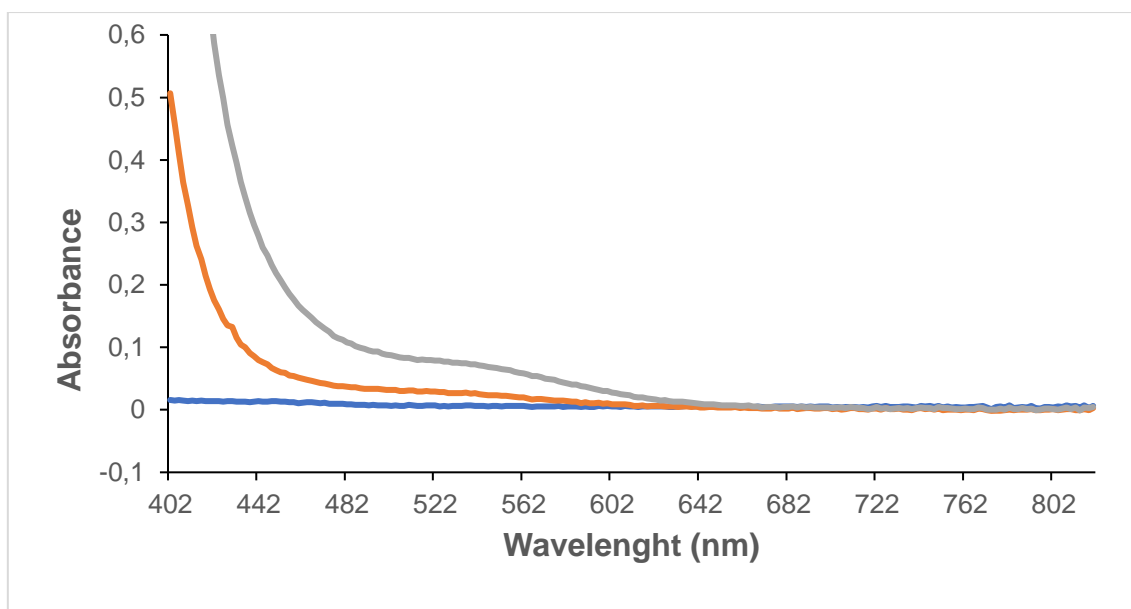The results obtained in both cases are displayed in Figure 12.

a)
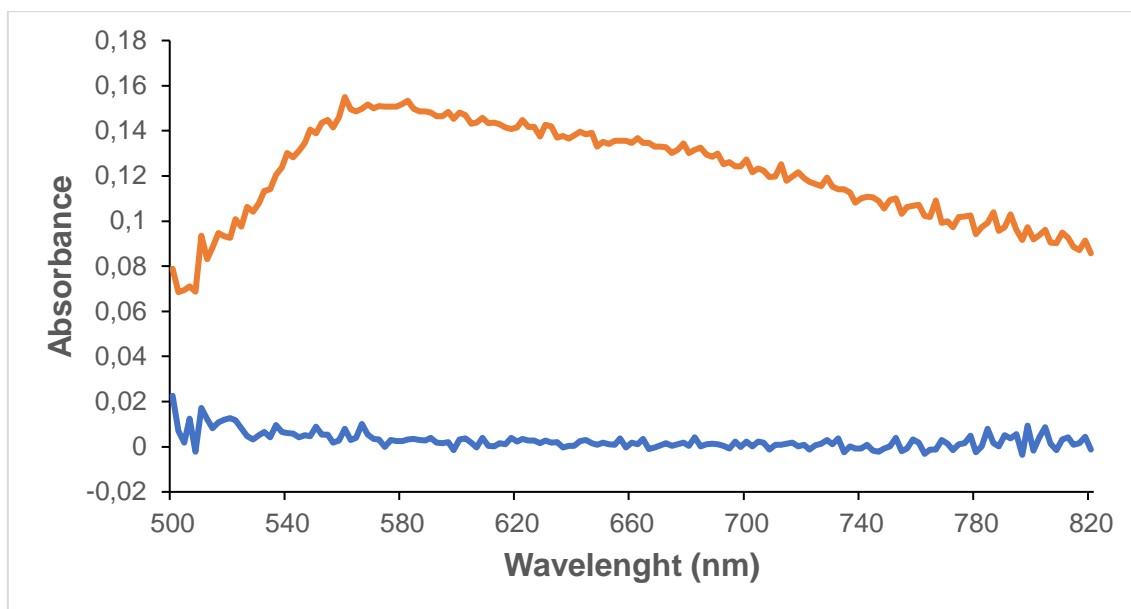
b)

Figure 12. UV-vis spectral changes for a) the photocatalytic oxidation of complex **2** (1 mM) in the presence of $[Ru^{III}(bpy)_3]^{2+}$ (0.5 mM), $[Na_2O_8S_2]$ (5.0 mM). Blue line: before photoirradiation and orange line: after 10 min of photoirradiation ($\lambda > 420$ nm), and b) the chemical oxidation of 2 (1.0 mM; blue line) by adding CAN (2.0 mM; orange line) and by adding CAN (4.0 mM; grey line), in a deareated acetate buffer (pH 4.0, 50 mM) and MeCN (v/v 1:6) mixed solvent at RT.

The UV/Vis spectra of solutions of **4** are featureless, in both cases as expected for MnII species. Addition of $[Ru^{II}(bpy)_3]^{2+}$ with irradiation (Figure 12 a) or Ce(IV) (Figure 12 b) causes the occurrence of new bands in the visible region at 560 nm and 640 nm (sholder) in the first case, and 550 nm in the second one. These values are in accordance with the formation of Mn(III) and Mn(IV) species.[14] With the idea to have more information about these species, ESI-MS experiments were tested. The formation of high manganese in acetate tampon, by the generated $[Ru^{III}(bpy)_3]^{3+}$ was confirmed by the ion peaks at m/z 439, 523, 530, 703 and 719, which mass and isotope distribution patterns of peaks correspond to $[Mn^{III}(phen)(CF3SO3)(HCN)]^+$, $[Mn^{IV}(O)(OH)(phen)2(H2O)]^+$, $[Mn^{III}(phen)_2(OH)_2(CH_3CN)]^+$, $[Mn^{III}(phen)(CF3SO3)(HCN)]^+$ and $[Ru^{II}(bpy)_3(CF3SO3)]^+$. In the case of use Ce(IV) the formation of ion peaks at m/z 523 and 703 was also detected. This is illustrated in Figure 13.

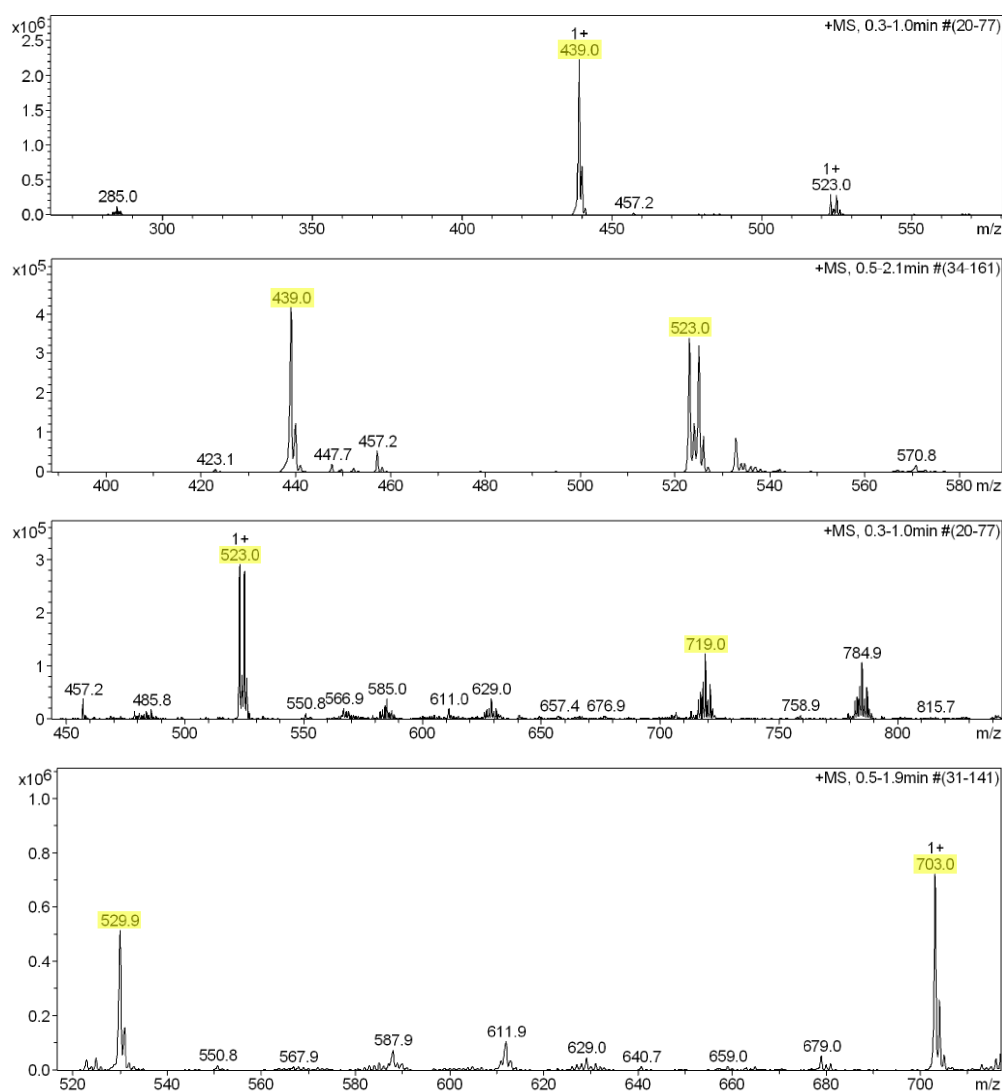**Figure 13.** ESI-MS spectra of compound 4's photoirradiation. Peaks at m/z 439, 523, 530, 703 and 719, which belong to high manganese species, are highlighted.

In base to the above described a proposed photocatalytic cycle for the oxidation of alcohols is shown in Figure 14.
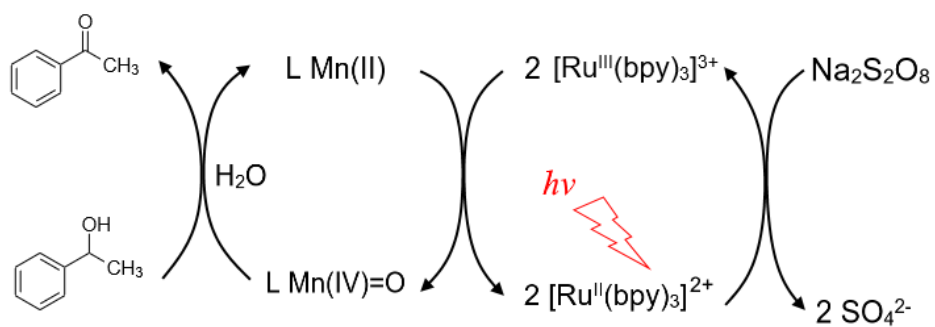

Figure 14. Steps involving the photooxidation of 1-phenyl ethanol by Mn^{II} complexes.

Chapter 5. Conclusions

1. Five manganese complexes (**1-5**) containing *dmp*, chloride and triflate ligands have been synthesized and characterized by spectroscopic, structural, analytical and electrochemical techniques. Complexes 1, **2** and **4** were obtained directly by mixing the reagents, stirring, filtrating the medium, and washing. Crystallization of compound **2** mother liquor gave rise to compound **3**. Recrystallization of complex **4** in an ethyl acetate solution produced crystals of **5**.

2. Structural analysis show that complex **1** presents an octahedral type of coordination, complex **2** is a dimer where the two manganese atoms are bridged by two chloride ligands, **3** has the structure of a distorted trigonal bipyramid, **4** displays a distorted trigonal prismatic geometry with visible stacking, and **5** shows a highly distorted octahedral coordination geometry around the Mn(II).

3. The electrochemical properties of complexes **1**, **2** and **4** have also been studied by cyclic voltammetry. Compounds **1** and **2** display one-electron quasi-reversible oxidation processes corresponding to the Mn^{III}/Mn^{II} system and, **4** shows an irreversible behavior. This compound is oxidised at a higher potential than the structurally similar chlorido complex **1**, which can be explained in terms of the stronger electron-donating capacity of chlorido ligands.

4. Compounds **1**, **2**, **4** were tested along with **1a**, **2a** and **3a** -synthesized in a previous study- in the photooxidation of alcohols into the corresponding aldehydes or ketones. All the compounds tested show moderate yields with high selectivity values. The complexes containing the pyridine pyrazole ligand present better performance than the complexes containing the *dmp* ligand and in general, the yield values displayed by chloride catalysts are higher than those presented by the triflate complexes. In addition, it was observed that changing the pH 6.8 buffer for a pH 4.0 slightly improved the yields.

5. Finally, UV-Vis and ESI-MS spectroscopy were performed to demonstrate that $[Mn^{II}(CF_3SO_3)_2(dmp)_2]$ complex is oxidized into Mn^{III} and Mn^{IV} species when is oxidized by a compound with a higher redox potential such as $[Ru^{III}(bpy)_3]^{3+}$. These results can evidence that high-valent species of Mn(IV) or Mn(III) are the active species responsible of the photooxidation of alcohols.

Bibliography

[1]   Lippard, S. J., Berg, J. M. (1994). *Principles of Bioinorganic Chemistry*. (U. S. Books, Ed.). Mill Valley, California.

[2]   a) Ko, S. Y., Lee, A. W. M., Masamune, S., Reed, L. A., Barry Sharpless, K., & Walker, F. J. (1983). Total synthesis of the L-hexoses. *Science*, *220*(4600), 949-951. doi: 10.1126/science.220.4600.949;

b) Nicolaou, K. C., Winssinger, N., Pastor, J., Ninkovic, S., Sarabia, F., He, Y., et al. (1997). Synthesis of epothilones A and B in solid and solution phase. *Nature*, *387*, 268-272. doi: 10.1038/387268a0;

c) Mark, H. F. (1986). *Encyclopedia of polymer science and engineering*. (J. I. Mark, H. F., Bikales, N. M., Overberger, C. G., Menges, G., Kroschwitz, Ed.), *Polymer* (2nd ed.). Weinheim: Wiley-VCH. doi: 10.1016/0032-3861(87)90274-6;

d) Darensbourg, D. J., Mackiewicz, R. M., Phelps, A. L., & Billodeaux, D. R. (2004). Copolymerization of CO 2 and epoxides catalyzed by metal salen complexes. *Accounts of Chemical Research*, *37*(11), 836-844. doi: 10.1021/ar030240u;

e) Jacobsen, E. N. (1993). *Catalytic Asymmetric Syntehsis*. (I. Ojima, Ed.). New Work: VCH.;

f) De Faveri, G., Ilyashenko, G., & Watkinson, M. (2011). Recent advances in catalytic asymmetric epoxidation using the environmentally benign oxidant hydrogen peroxide and its derivatives. *Chemical Society Reviews. 40***,** 1722-1760. doi: 10.1039/c0cs00077a

[3]   Crabtree, R. H. (2010). *Energy Production and Storage: Inorganic Chemical Strategies for a Warming World*. (R. H. Crabtree, Ed.) (1st ed.). John Wiley & Sons, Inc.

[4]   Esswein, A. J., & Nocera, D. G. (2007). Hydrogen production by molecular photocatalysis. *Chemical Reviews*, *107*(10), 4022-4047. doi: 10.1021/cr050193e

5   Wu, X., Yang, X., Lee, Y. M., Nam, W., & Sun, L. (2015). A nonheme manganese(iv)-oxo species generated in photocatalytic reaction using water as an oxygen source. *Chemical Communications*, *51*(19), 4013-4016. doi: 10.1039/c4cc10411k

6   Zhou, D. F., Chen, Q. Y., Qi, Y., Fu, H. J., Li, Z., Zhao, K. Di, & Gao, J. (2011). Anticancer activity, attenuation on the absorption of calcium in mitochondria, and catalase activity for manganese complexes of N-substituted Di(picolyl)amine. *Inorganic Chemistry*. doi: 10.1021/ic200004y

7   Anastas, P., Warner, J. (1998). *Green Chemistry: Theory and Practice*. (O. U. Press, Ed.). Oxford.

8   Manrique, E. (2018). *Development of New Transition Metal Complexes for their Use in Sustainable Catalytic Processes and as Antitumoral Agents*. Universitat de Girona, Catalunya.

9   Lennartson, A. (2010). Co-crystallizing coordination compounds. *Journal of Coordination Chemistry*, *63*(20), 4177-4187. doi: 10.1080/00958972.2010.535145

10   Romero, I., Collomb, M. N., Deronzier, A., Llobet, A., Perret, E., Pécaut, J., et al (2001). A novel dimanganese(II) complex with two chloride bridges - A two-electron oxidation system. *European Journal of Inorganic Chemistry*, *2001*(1), 69-72. doi: 10.1002/1099-0682(20011)2001:1<69::AID-EJIC69>3.0.CO;2-6

11   Rich, J., Rodríguez, M., Romero, I., Vaquer, L., Sala, X., Llobet, A., et al (2009). Mn(ii) complexes containing the polypyridylic chiral ligand (−)-pinene[5,6]bipyridine. Catalysts for oxidation reactions. *Journal of the Chemical Society. Dalton Transactions*, *2009*(38), 8117-8126. doi: 10.1039/B906435D

12   Van Gorkum, R., Buda, F., Kooijman, H., Spek, A. L., Bouwman, E., & Reedijk, J. (2005). Trigonal-prismatic vs. Octahedral geometry for MnII Complexes with innocent didentate ligands: A subtle difference as shown by XRD and DFT on [Mn(acac)2(bpy)]. *European Journal of Inorganic Chemistry*, *2005*(11), 2255-2261. doi: 10.1002/ejic.200401005

13   Hureau, C., Blondin, G., Charlot, M. F., Philouze, C., Nierlich, M., Césario, M., & Anxolabéhère-Mallart, E. (2005). Synthesis, structure, and characterization of new mononuclear Mn(II) complexes. Electrochemical conversion into new oxo-bridged Mn 2(III,IV) complexes. Role of chloride ions. *Inorganic Chemistry*, *44*(10), 3669-3683. doi: 10.1021/IC050243Y

14   Wu, X., Yang, X., Lee, Y. M., Nam, W., & Sun, L. (2015). A nonheme manganese(iv)-oxo species generated in photocatalytic reaction using water as an oxygen source. *Chemical Communications*, (51), 4013-4016. doi: 10.1039/C4CC10411K